Arabian Journal of Geosciences (2022) 15: 816
https://doi.org/10.1007/s12517-022-10047-z

ORIGINAL PAPER

Chemometric differentiation of crude oils and their inferred source rocks in Halfaya, Amara, and Noor oilfields, southern Iraq

Mohamed W. Alkhafaji[1] · Sawsan H. Al-Hazaa[1] · Kenneth Peters[2]

Received: 27 December 2021 / Accepted: 1 April 2022 / Published online: 20 April 2022

Abstract

Oil samples from the Halfaya, Noor, and Amara oilfields were geochemically characterized to determine their origin, type of organic matter, and the depositional environment conditions of the correlative source rocks. Detailed saturated and aromatic biomarkers from nine oil samples were analyzed using gas chromatography and gas chromatography-mass spectrometry, and measurement of sulfur content and stable carbon isotopes. Saturated hydrocarbons in the oil samples are low, whereas polar fractions are relatively high. Saturated (terpane and sterane) and aromatic biomarker ratios suggest that these oil samples were generated mainly from early to mid-mature carbonate source rocks. The anoxic marine depositional environment of the source rocks is reflected by the high $C_{35}S/C_{34}S$ hopane and low Pr/Ph ratios. Hierarchical cluster analysis (HCA) identifies two oil families. These oil families may have originated from the same source rock but with different organofacies. Regular sterane distributions differ from those for oils from the southern oilfields (Majnoon, Nasiriah, West Qurna, North Rumaila, Luhais, Abu Gharab, Faka, Buzergan). Biomarker ratios indicate that the present study oils are slightly more mature than southern oils and their source rock depositional environment was more reducing (anoxic). Based on comparison with previously published data, the most likely source rocks for the present study oils include the Sulaiy, Yamama, and Zubair formations.

Keywords Biomarker · Organic geochemistry · Halfaya · Noor · Amara · Chemometric analysis

Introduction

Iraq is the main oil producing country in the world with proven reserves of about 113 billion barrels of oil (BBO) (Verma et al. 2004), and an additional 43 BBO from the Kurdistan Region (Abdula 2010). Five petroleum systems were recognized (Jassim and Al-Gailani 2006; Aqrawi et al. 2010). A Paleozoic petroleum system in western Iraq is based mainly on Silurian Hot Shale of the Akkas Formation (Verma et al. 2004; Alkhafaji et al. 2015a, b) and Carboniferous Ora Formation (Alkhafaji 2017; 2018). A Triassic petroleum system is based on the Triassic Kurra Chine Formation in northwestern Iraq. A Jurassic petroleum system is based on Sargelu and Naokelekan formations as source rocks where the Gotnia Formation anhydrite is the main seal rock. A Cretaceous petroleum system, which is the most important, is based mainly on the Chia Gara and Sulaiy formations as the main source rocks where the Mishrif, Nahr Umr, Khasib, and Qamchuqa formations are the main reservoirs. A Cenozoic petroleum system is based on the Eocene Aaliji Formation as source rock and the Miocene Fat'ha Formation as the main seal rock.

Most oils in Iraq were discovered in Cretaceous, Paleogene, and Neogene reservoirs in the Zagros Fold Belt Zone and Mesopotamian Basin (Alsharhan and Nairn 1997; Jassim and Al-Gailani 2006; Abeed et al. 2012; Al-Khafaji et al. 2018). The Mesopotamian Basin is the most important oil provinces in Iraq; it contains several supergiant and giant oilfields (Fig. 1); therefore, it has been the subject of several studies. Some of these studies focused on source rocks (Abeed et al. 2011; Al-Ameri and Al-Musawi 2011; Idan et al. 2015); while others focused on petroleum geochemistry (Abeed et al. 2012; Al-Ameri et al. 2014; Al-Marsomy and Al-Ameri 2015; Hakimi and Najaf 2016; Hasan and Al-Dulaimi 2017; Al-Khafaji et al. 2018; 2021). These studies

Responsible Editor: Santanu Banerjee

✉ Mohamed W. Alkhafaji
mohamed_wagga@yahoo.com

[1] Applied Geology Department, College of Science, University of Tikrit, Tikrit, Iraq

[2] Department of Geological and Environmental Sciences, Stanford University, Stanford, CA, USA

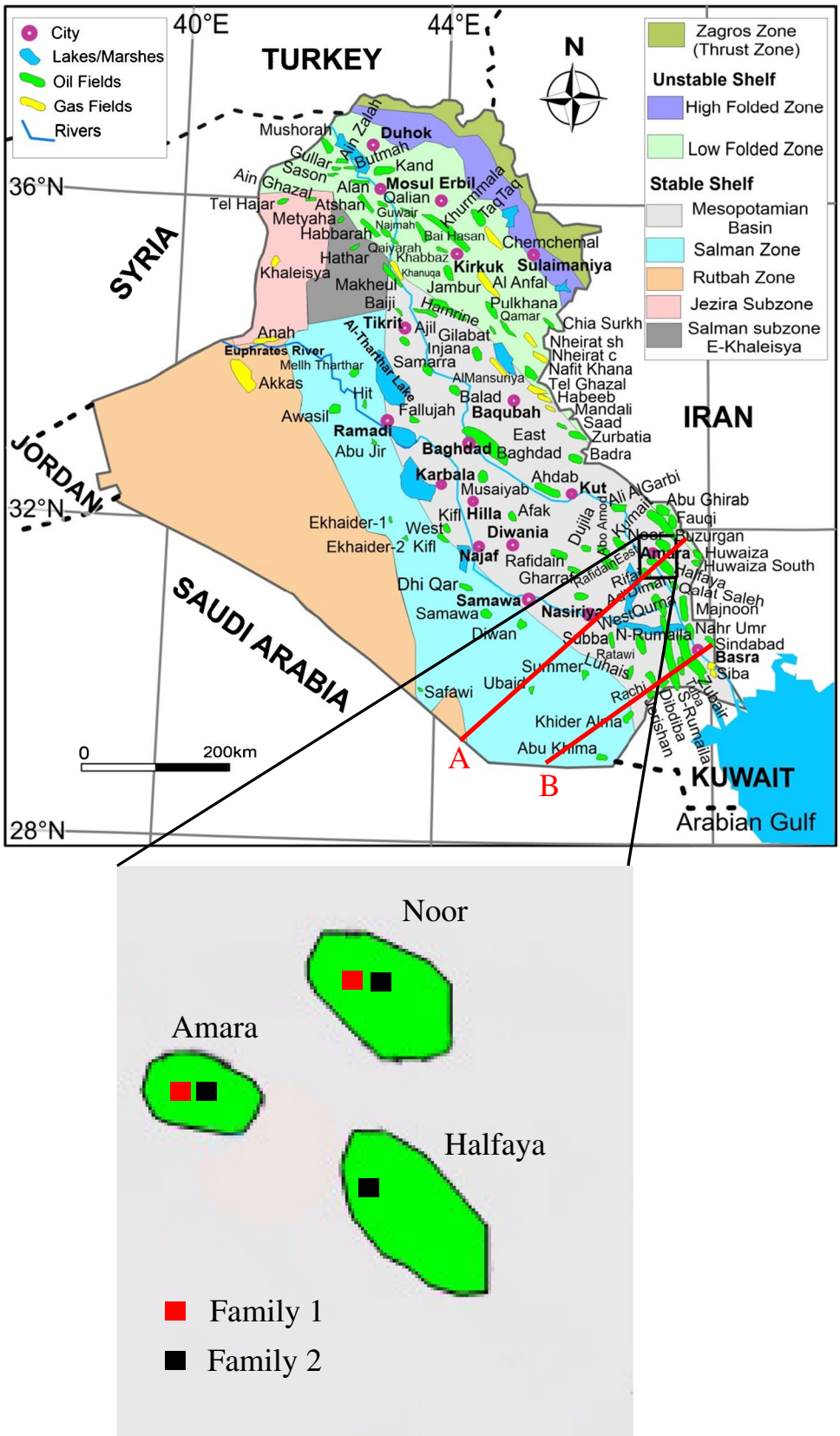

Fig. 1 Map of Iraq showing the petroleum fields (top) and the location of the studied oilfields (bottom) (after Mohamed, 2021)

suggested that source rocks in the Mesopotamian Basin of southern Iraq are mostly Jurassic (Tithonian)-Cretaceous units. This study aims to evaluate the molecular composition of the oils in the Halfaya, Amara, and Noor oilfields, in order to group them geochemically and to determine the conditions of the depositional environment of their corresponding source rocks.

Geological setting

Tectonically, the study area oilfields are located in the Mesopotamian Zone of the Stable Shelf (Fig. 1). The sedimentary cover of this zone comprises of 2500–5000 m of Paleozoic, 3800–5400 m of Mesozoic, and 350–2400 m of Tertiary and Quaternary sediments (Jassim and Buday 2006a). The sedimentary cover thickens eastward (Fig. 2). It also contains buried faulted structures with mainly northwest-southeast trends, separated by broad synclines (Jassim and Buday 2006b).

Continental collision between Arabian Plate and Eurasia Plate in the Late Cretaceous led to formation of a foredeep basin named the Mesopotamian Basin (Ameen 1992). This zone is mildly folded and the pre-Neogene folds in the southern part of this basin are broad with north–south orientation. During the Middle Jurassic, renewed extension along the northeast margin of the Arabian Plate resulted in a restricted intrashelf basin (Gotnia Basin) that covered most of eastern Iraq (Aqrawi et al. 2010). The euxinic Iraqi portion of this basin was separated from open marine waters by barriers (Jassim and Buday 2006a, b, c, d). During the Middle Jurassic, deposition in these basins occurred in a restricted and deep water environment and is represented by bitumineous carbonate and shales of the Sargelu Formation (Fig. 3) (Jassim and Buday 2006a, b, c, d). The Sargelu Formation was followed by deposition of high energy shoal carbonate of the Najmah Formation. During Late Kimmeridgian-Early Tithonian time, the basin became more evaporitic resulting in deposition of the Gotnia evaporites, which are the main cap rocks in the basin (Alsharhan and Nairn 1997).

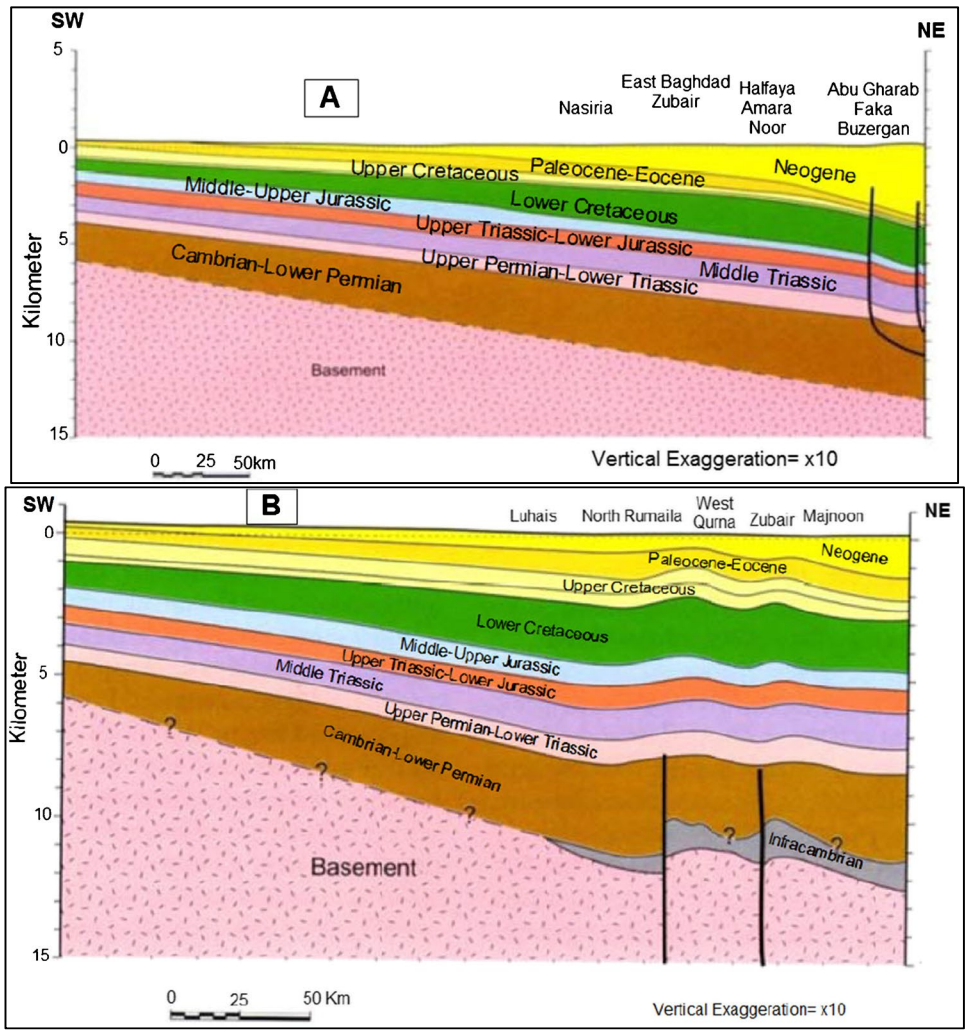

Fig. 2 SW-NE cross sections along profiles **A** and **B** (shown in Fig. 1) show the locations of the studied and neighboring oilfields (modified after Aqrawi et al. 2010)

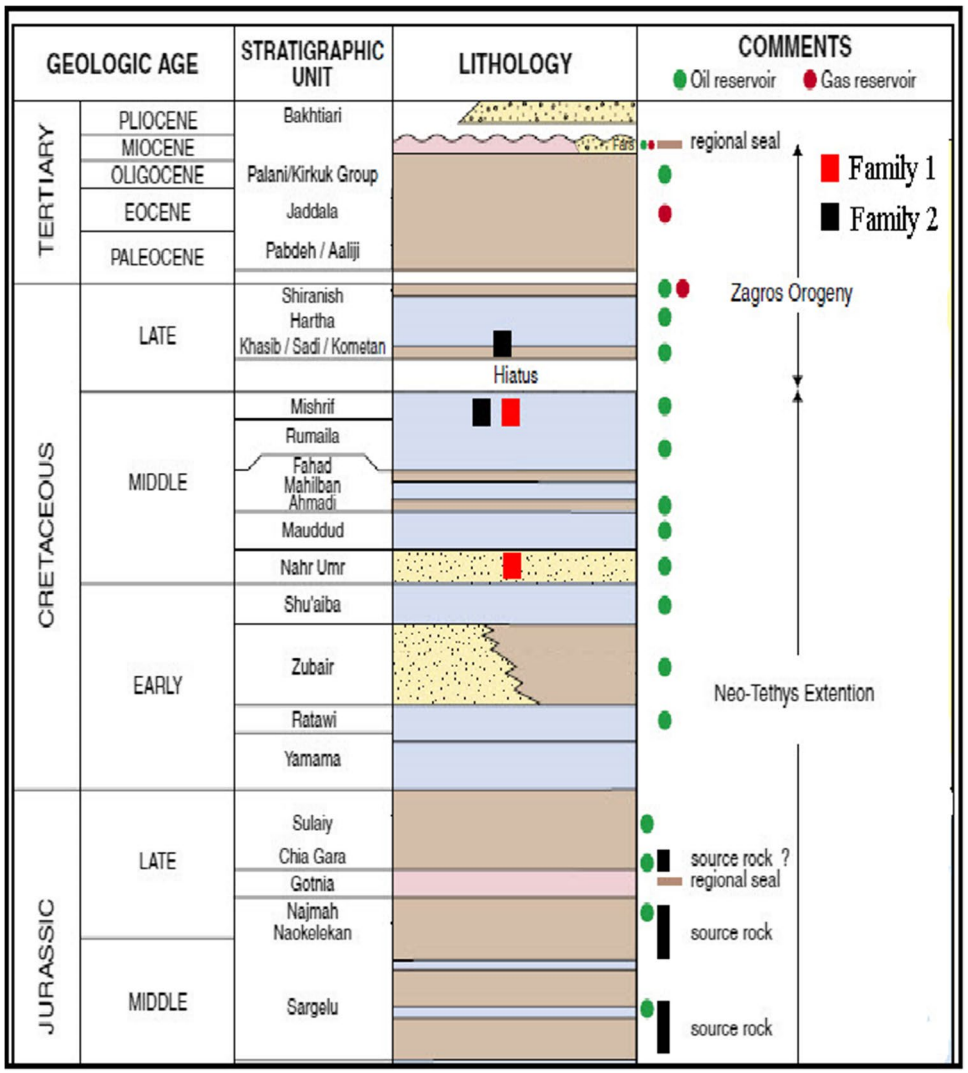

Fig. 3 Stratigraphic section and Mesozoic-Cenozoic petroleum system elements (after Pitman et al. 2004)

Late Jurassic sequences (Najmah and Gotnia) are thickest in the Mesopotamian and Salman zones (> 700 m). During Late Tithonian-Valanginian time, neritic carbonates of the Sulaiy Formation were deposited in the Salman Zone and some parts of the Mesopotamian Zone (Jassim and Buday 2006a, b, c, d). Shallow water carbonate and outer shelf marl were deposited in the Mesopotamian Zone due to repeated cycles of transgression and regression beginning with the Sulaiy and Yamama formations and ending with the Ratawi Formation (Jassim and Buday 2006a, b, c, d). Clastic sediments of the Zubair Formation, which is main oil reservoir in the Mesopotamia Zone, were deposited on the southwest shoreline of the basin in littoral environments during the Barremian-Aptian marine regression followed by deposition of Shu'aiba Formation on a carbonate ramp during marine transgression.

Clastic facies of the Nahr Umr Formation, which is also a main oil reservoir rock in the Mesopotamian Zone (Fig. 3), were deposited in the Mesopotamian and Salman zones on the inner shelf during the Albian (Jassim and Buday 2006a, b, c, d). The Nahr Umr Formation is overlain by carbonate shelf sediments of the Mauddud Formation. Reactivation of longitudinal ridges (such as the Mosul High) occurred due to deformation along the northeast Tethyan margin of the Arabian Plate during Cenomanian-Early Turonian time (Jassim and Buday 2006a, b, c, d). On the shelf, the main basin was divided into small basins by northwest-southeast ridges, which led to major facies variations. Limestones and marls of the Rumaila Formation were deposited in a deep inner-middle shelf setting. Within the Rumaila basin, shoals and patch reefs of the Mishrif Formation, which is also main oil-bearing formation in the Mesopotamian Basin, were deposited on actively growing structures (Al-Nqar et al. 2019; Taha and Abdullah 2020). Carbonate and clastic facies of the inner shelf (Ahmadi Formation) were deposited in shallow marine basins in the south of Iraq. In the Mesopotamian Zone, the Khasib, Tanuma, and Sa'adi formations were deposited in deep inner shelf and lagoonal

environments during Turonain-Early Campanian time (Jassim and Buday 2006a, b, c, d).

From the late Cretaceous to Miocene, intrashelf basins were filled progressively with marine carbonate and shales. Shallow marine carbonate (limestone and dolomite) sedimentation was dominant from Eocene to early Miocene. During the Middle Miocene, thick evaporites (Fat'ha Formation) were deposited in restricted sub-basins, which act as regional seal rocks for most of the Tertiary reservoirs in Iraq. Late Miocene and Pliocene time represents the transition from marine to continental sedimentation. Subsequently, thick clastic beds of claystone, sandstone, and conglomerates were deposited in a foredeep basin and finally filled the basin.

Materials and methods

For this study, nine crude oil samples from Cretaceous reservoirs in the Halfaya, Amara, and Noor oilfields in Messan Province in southern Iraq were collected for detailed organic geochemical study (Fig. 1; Table 1).

For biomarker analyses, about 1 g of each oil sample was used. The asphaltenes were precipitated by adding hexane, and then the deasphalted soluble fraction was fractionated into three fractions: saturated hydrocarbons, aromatic hydrocarbons, and resin on a silica column by elution with *n*-pentane, *n*-pentane-dichloromethane, and methanol (CH_3OH). After concentration, the solvent, the gas chromatography, and gas chromatography–mass spectrometry instruments were used to analyze the saturated and aromatic biomarkers of these samples.

A Costech elemental analyzer was used for the stable carbon isotope compositions of C15 + saturated and C15 + aromatic hydrocarbons. Pirouette v. 4.5 rev. 1 (Infometrix, Inc.) was used for cluster and principal component analyses.

Result and discussion

Bulk composition

All Halfaya, Noor, and Amara oil samples have relatively high aromatic hydrocarbon contents (38.20–46.81%) and moderate amounts of saturates (17.26–34.83%) and polars (23.55–44.54%) (Table 1). In addition, they exhibit relatively high sulfur content (2.47–5.60%). The relatively high sulfur and polar contents could indicate that they are biodegraded. But the high abundance of normal alkanes and isoprenoids in the oil samples reduces the possibility of biodegradation. In addition, the low values of Pr/*n*-C_{17} and Ph/*n*-C_{18} (Table 2 and Fig. 4) indicate that Halfaya, Amara, and Noor oil samples are not biodegraded.

Table 1 Bulk composition and carbon isotope values for the Halfaya, Amara, and Noor oil samples

Well	Reservoir	Depth (m)	Oil family	< C15%	%S	%Sat	%Aro	%NSO	%Asph	%Polars	δ13Cw.s ‰	δ^{13}Cs ‰	δ^{13}Ca‰	CV
Noor-13	Nahr Umr	4123	1	34.74	2.62	33.33	40.13	17.80	8.74	26.54	− 27.46	− 28.12	− 27.52	− 1.61
Amara-6	Nahr Umr	3700	1	32.02	2.47	34.83	41.62	16.47	7.08	23.55	− 27.52	− 28.23	− 27.53	− 1.34
Amara-5	Mishrif	2820	1	32.04	2.49	34.89	41.02	17.23	6.86	24.09	− 27.63	− 28.16	− 27.52	− 1.50
Halfaya-18	Mishrif	3433	2	13.30	5.30	20.57	40.07	21.76	17.60	39.36	− 27.42	− 27.53	− 27.40	− 2.81
Halfaya-119	Mishrif	3130	2*	13.81	5.35	19.67	41.99	17.57	20.77	38.34	− 27.38	− 27.28	− 27.44	− 3.54
Halfaya-133	Mishrif	3445	2	14.76	5.37	19.59	41.46	14.69	24.26	38.95	− 27.43	− 27.50	− 27.36	− 2.81
Halfaya-272	Mishrif	3225	2	14.72	5.60	17.26	38.20	18.04	26.50	44.54	− 27.44	− 27.53	− 27.44	− 2.94
Noor-6	Mishrif	3473	2	28.15	5.43	19.52	44.70	17.82	17.96	35.79	− 27.37	− 27.66	− 27.35	− 2.40
Amara-5	Khasib	2831	2	29.10	4.29	22.67	46.81	17.33	13.19	30.52	− 27.24	− 27.34	− 27.35	− 3.19

δ13Cw.s ‰, carbon isotope of the whole sample; *CV*, canonical variable (Sofer, 1984); $\delta^{13}Cs$ ‰, carbon isotope of the saturate fraction; $\delta^{13}Ca‰$, carbon isotope of the aromatic fraction; *outliner in family 2

Table 2 Normal alkanes and isoprenoid parameters for the Halfaya, Amara, and Noor oil samples

Well	Depth (m)	Oil family	Pr/Ph	Pr/n-C_{17}	Ph/n-C_{18}	n-C_{27}/n-C_{17}	CPI
Noor-13	4123	1	0.68	0.14	0.23	0.21	0.96
Amara-6	3700	1	0.67	0.14	0.23	0.22	0.99
Amara-5	2820	1	0.67	0.14	0.24	0.22	0.99
Halfaya-18	3433	2	0.66	0.16	0.27	0.20	0.96
Halfaya-119	3130	2*	0.66	0.16	0.27	0.19	0.98
Halfaya-133	3445	2	0.69	0.17	0.28	0.19	0.98
Halfaya-272	3225	2	0.67	0.16	0.27	0.19	0.97
Noor-6	3473	2	0.68	0.16	0.27	0.19	0.99
Amara-5	2831	2	0.70	0.14	0.22	0.19	0.95

*Outliner in family 2; *CPI*, carbon preference index

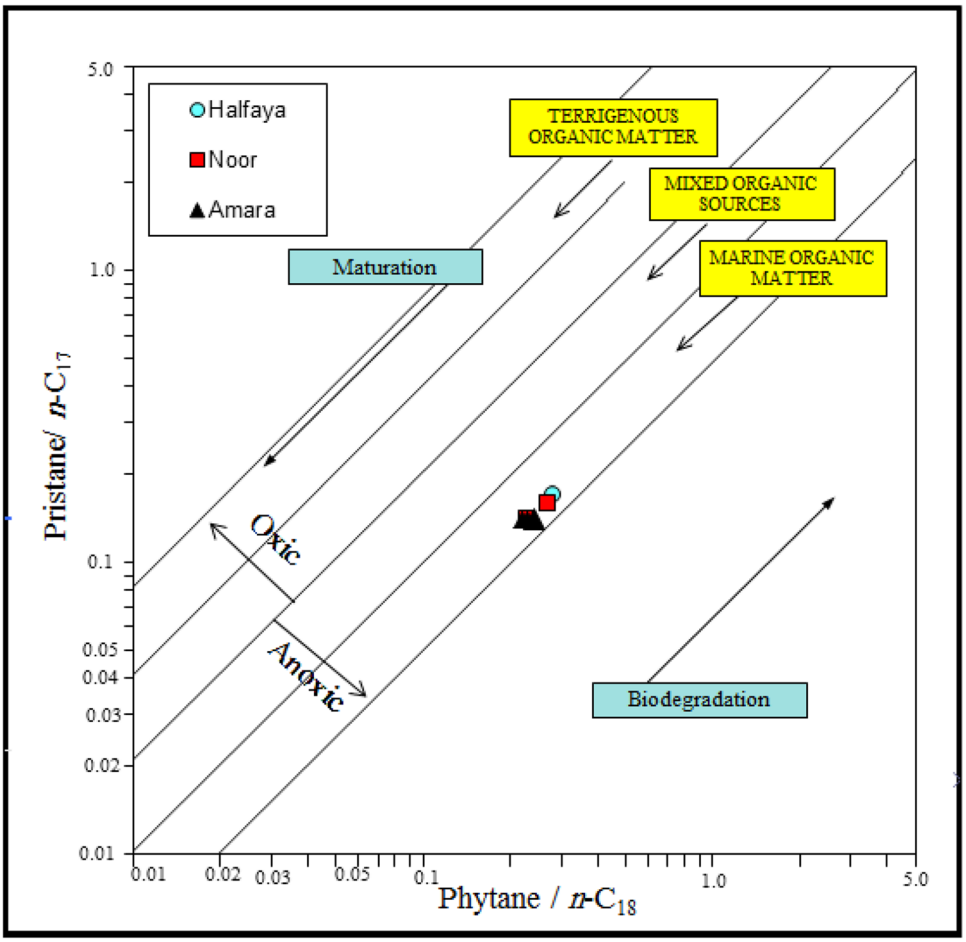

Fig. 4 Pr/n-C_{17} versus Ph/n-C_{18} can be used to infer the type of organic matter in source rocks for the Halfaya, Amara, and Noor oils

High sulfur is associated with high asphaltene content (Table 1). Generally, Halfaya samples show higher sulfur and asphaltene contents, and low content of low molecular-weight hydrocarbons (LMWH). The low content of LMWH of Halfaya samples led to reduced API gravity in comparison with samples from other oilfields. API gravity values of Halfaya oils rise from 21 to 26° in Mishrif reservoir to 38° in the Nahr Umr reservoir (Al-Ameri et al. 2014).

Source of organic matter and depositional environment

The terpane, steranes, and aromatic biomarkers used to interpret the depositional environment of the corresponding source rocks are listed in Table 3. The narrow range of all sterane and terpane biomarker ratios indicates that all oil samples have a common source. As mentioned above, the sulfur content of all oil samples is relatively high, suggesting

an anoxic carbonate depositional environment for their source rocks containing type II or type II-S kerogen (Tissot and Welte 1984; Peters et al. 2005).

Gas chromatograms (GC) show unimodal distributions of normal alkanes with carbon numbers in the range C_8–C_{35}, peaking at C_{14}–C_{16} in the Halfaya oil samples, and C_9–C_{11} in the Noor and Amara samples (Fig. 5). A dominance of short-chain over long-chain *n*-alkanes (*n*-C_{27}/*n*-C_{17} between 0.19 and 0.22; Table 2) indicates a high contribution of marine organic matter (Peters et al. 2005). Carbon preference indices (CPI) for the oil samples are 1.04–1.19 (Table 2), indicating slight odd-over-even predominance (Bray and Evans 1961). Moreover, the contribution of marine algae is indicated by the presence of C_{30} steranes (24-n-propylcholestane) (Moldowan et al.1990) (Fig. 6). This interpretation is supported by low Pr/*n*-C_{17} and Ph/*n*-C_{18} values (Table 2), canonical variable (CV) (< − 1.5; Table 1), and carbon isotope values (Table 1 and Fig. 7) (Sofer 1984). The Pr/Ph ratio for all samples is < 0.70 (Table 2), suggesting that the source rocks for these oils were deposited under anoxic conditions (Didyk et al. 1978). This suggestion is supported by the high $C_{35}S/C_{34}S$ homohopane values in all oil samples (> 1.07) (Table 3; Fig. 8), and relatively high homohopane index values (0.13–0.15; Table 3) (Peters and Moldowan 1991). Gammacerane is present in low concentrations, with Ga/C_{30} hopane ratios for all samples < 0.1 (Table 3); indicating that the source rocks were not deposited under stratified water conditions (Sinninghe Damste' et al. 1995; Jiang and George 2020). In addition, the high bacterial contribution is indicated by the low sterane/hopane ratios (< 0.27, Table 3) (Rohmer et al. 1992).

Mass chromatograms of the terpanes of the oil samples show that C_{27}–C_{35} hopanes are present in all oil samples, dominated by C_{29} hopane followed by C_{30} hopane. Tricyclic terpanes (C_{19}–C_{29}) are present in low abundance relative to hopanes (Fig. 8). Tricyclic and tetracyclic terpanes are source parameters (Peters et al. 2005; Burton et al. 2019). High abundance of C_{24} tetracyclic terpanes and high C_{24} tetracyclic terpane/C_{23} tricyclic terpane ratio (> 1.29; Table 3) suggest carbonate source rocks (Palacas 1984; Clark and Philp 1989). The carbonate source rock assumption is supported by the low C_{24}/C_{23}, high C_{22}/C_{21} tricyclic terpanes (Table 3) (Waples and Machihara 1991), high C_{30} norhomohopane/C_{30} hopane (0.18–0.25), and low C_{27} diasteranes/regular steranes (< 0.21; Table 3) and Ts/Tm ratios (< 0.25; Table 3). The C_{29}/C_{30} hopane ratios for the oil samples are high (> 1.32, Table 3), further indicating carbonate source rocks (Zumberge 1984). High dibenzothiophene/phenanthrene (DBT/P) (Table 3) and low Pr/Ph values also demonstrate that these oils were generated from marine carbonate or marl source rocks (Hughes et al. 1995) (Fig. 9). On the other hand, Wang and Fingas (1995) reported that methyldibenzothiophene (MDBT) distributions for oil

Table 3 Source-related biomarker ratios for the Halfaya, Amara, and Noor oil samples

Well	Oil family	C_{19}/C_{23}	C_{22}/C_{21}	C_{24}/C_{23}	Tet/C_{23}	H.I	C_{29}/H	Ga/H	$C_{35}S/C_{34}S$	S/H	Ts/Tm	$C_{30}NH/C_{30}H$	% C_{27}	% C_{28}	% C_{29}	Dia./Reg	DBT/P
Noor-13	1	0.17	0.94	0.31	1.68	0.11	1.32	0.06	1.07	0.26	0.24	0.19	32.78	23.61	43.61	0.21	2.18
Amara-6	1	0.19	0.90	0.32	1.68	0.12	1.32	0.07	1.12	0.26	0.25	0.19	33.04	24.03	42.93	0.21	2.53
Amara-5	1	0.19	0.97	0.30	1.69	0.11	1.34	0.07	1.07	0.26	0.25	0.18	32.17	24.37	43.47	0.20	2.49
Halfaya-18	2	0.12	1.11	0.26	1.34	0.12	1.66	0.09	1.13	0.18	0.18	0.25	32.76	24.44	42.80	0.11	2.95
Halfaya-119	2*	0.13	1.14	0.26	1.40	0.12	1.66	0.09	1.13	0.18	0.18	0.24	34.07	22.85	43.08	0.11	2.93
Halfaya-133	2	0.13	1.08	0.25	1.35	0.12	1.61	0.09	1.10	0.18	0.20	0.24	33.53	24.09	42.38	0.11	3.01
Halfaya-272	2	0.11	1.15	0.26	1.36	0.13	1.46	0.09	1.10	0.19	0.18	0.25	33.64	24.10	42.26	0.12	2.74
Noor-6	2	0.12	1.03	0.26	1.35	0.13	1.61	0.08	1.14	0.19	0.20	0.24	33.62	23.69	42.69	0.15	2.90
Amara-5	2	0.12	1.10	0.26	1.29	0.13	1.54	0.08	1.10	0.19	0.19	0.24	33.49	24.15	42.35	0.10	3.07

*Outliner in family 2; *H. I.*, Homohopane index (C_{35}/(C_{31} to C_{35}); *Ga/H*, Gammacerane/C_{30} hopane; *S/H*, Steranes/hopanes (Σ(C_{27}-C_{29}) steranes/ Σ hopanes); $C_{30}NH/C_{30}H$, C_{30} norhomohopane/C_{30} hopane; *Dia./Reg*, diasteranes/regular steranes; *DBT/P*, dibenzothiophene/phenanthrene

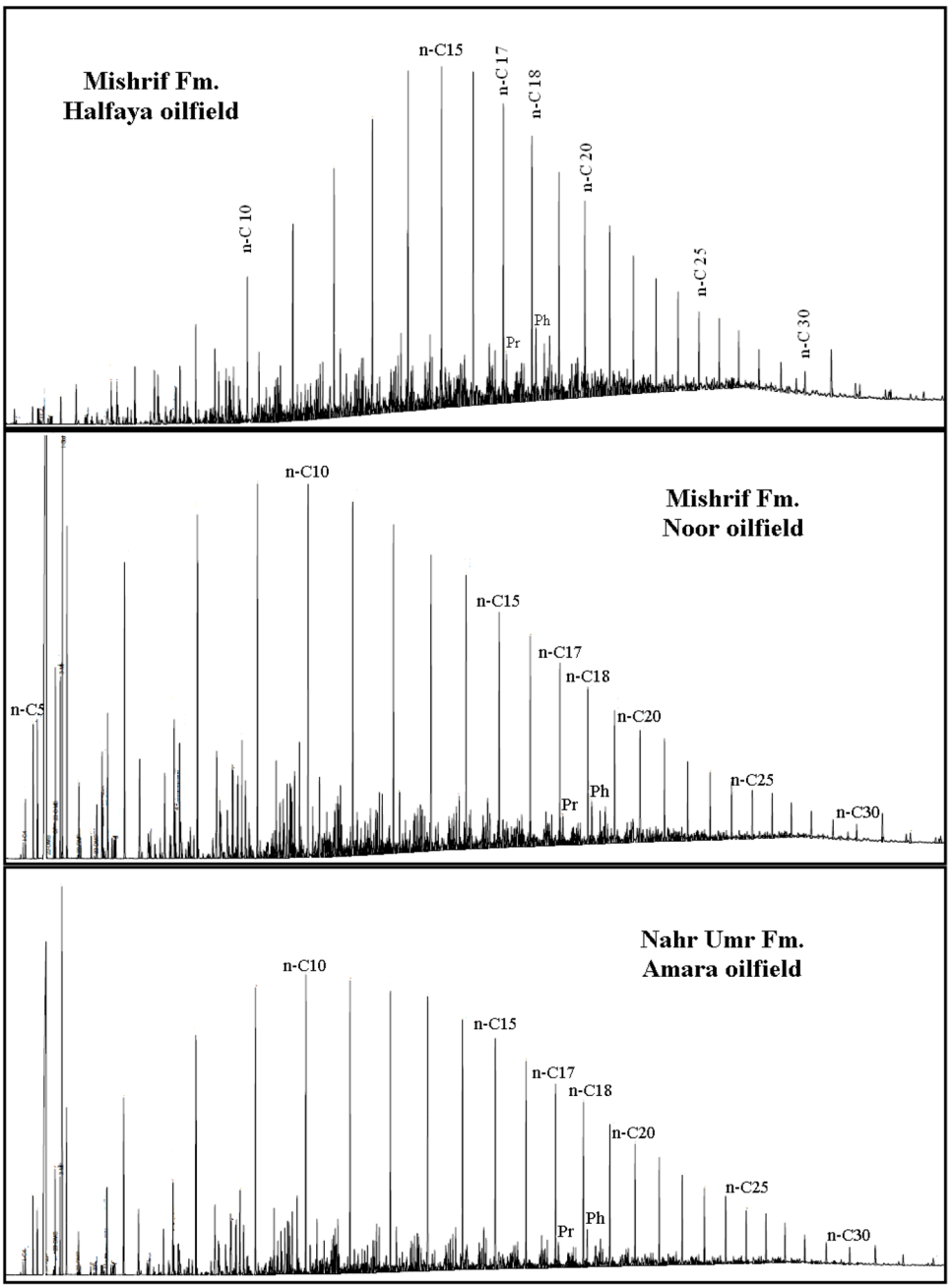

Fig. 5 Whole oil gas chromatograms showing the *n*-alkane distributions of some Halfaya, Amara, and Noor oils

generated from pure carbonate source rocks have V shapes (i.e., $4>2+3<1$). MDBT distributions for all oil samples in the present study are not consistent with those of pure carbonate rocks. Their abundance is in the following order: $4>2+3>1$ (Fig. 10). This distribution may result from some shale bed contribution to the source rocks. Indeed, all suggested source rocks in the Mesopotamian basin have interlayered shale beds.

The sterane distributions *(m/z* 217, Fig. 6) for the oil samples are similar and show C_{29} steranes are dominant (Fig. 6 and Table 3). In general, C_{29} steranes come from brown and green algae and from land plants (Volkman 2003), C_{27} steranes from marine algae, while C_{28} are from green algae and higher plants (Volkman 1986). In the oil samples of this study, there is no indication for high contribution from higher-plant organic matter to source rocks. Therefore, the C_{29} steranes of the oil samples may originate from microalgae, which contain a high concentration of C_{29} sterols (Volkman et al. 1999) and these may be the source of the C_{29} steranes in the oil samples. In addition, the sterane distributions of the oil samples show abundant pregnane and homopregnane (C_{21} and C_{22} steranes, Fig. 6). These compounds can be indicators for hypersaline depositional environments (Peters and Moldowan 1993), or restricted clastic-starved

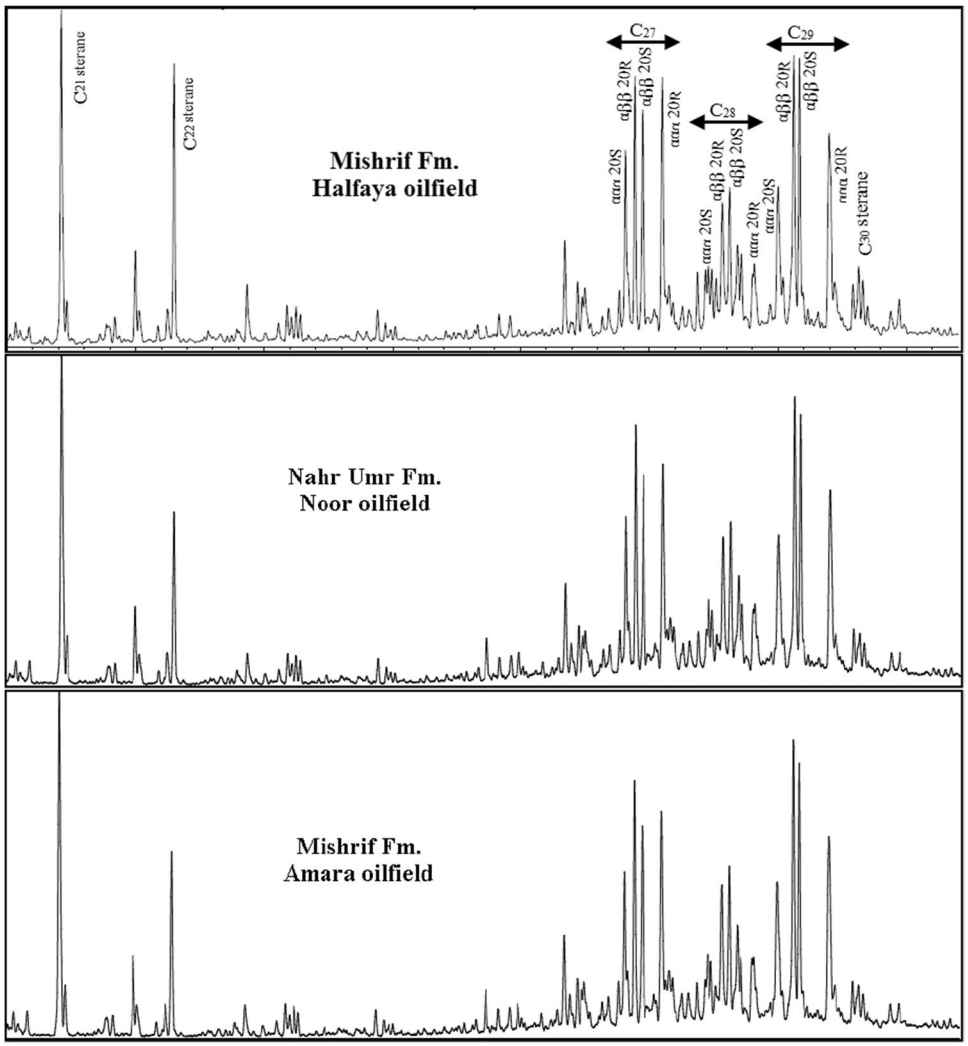

Fig. 6 *M/z* = 217 traces showing sterane distributions for some oil samples

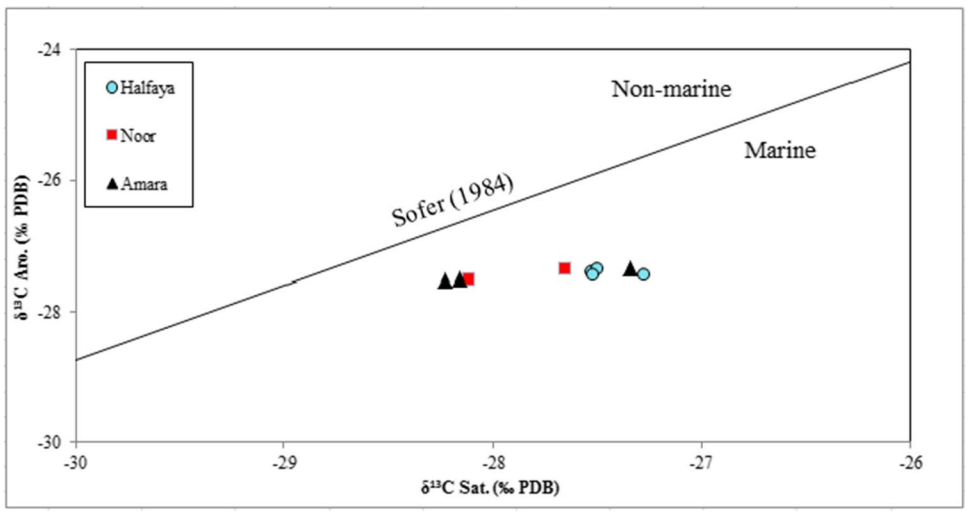

Fig. 7 $\delta^{13}C$ of saturated versus aromatic hydrocarbons showing the inferred type of organic matter in source rocks for the Halfaya, Amara, and Noor oil samples

depositional environments (Requejo et al. 1997). These compounds form preferentially (rather than diasteranes) under clay-poor anoxic conditions (Moldowan et al. 1985). The low diasterane abundance in the oil samples indicates that they were generated from carbonate source rocks deposited in an anoxic environment. Sulfurization of the steroid side

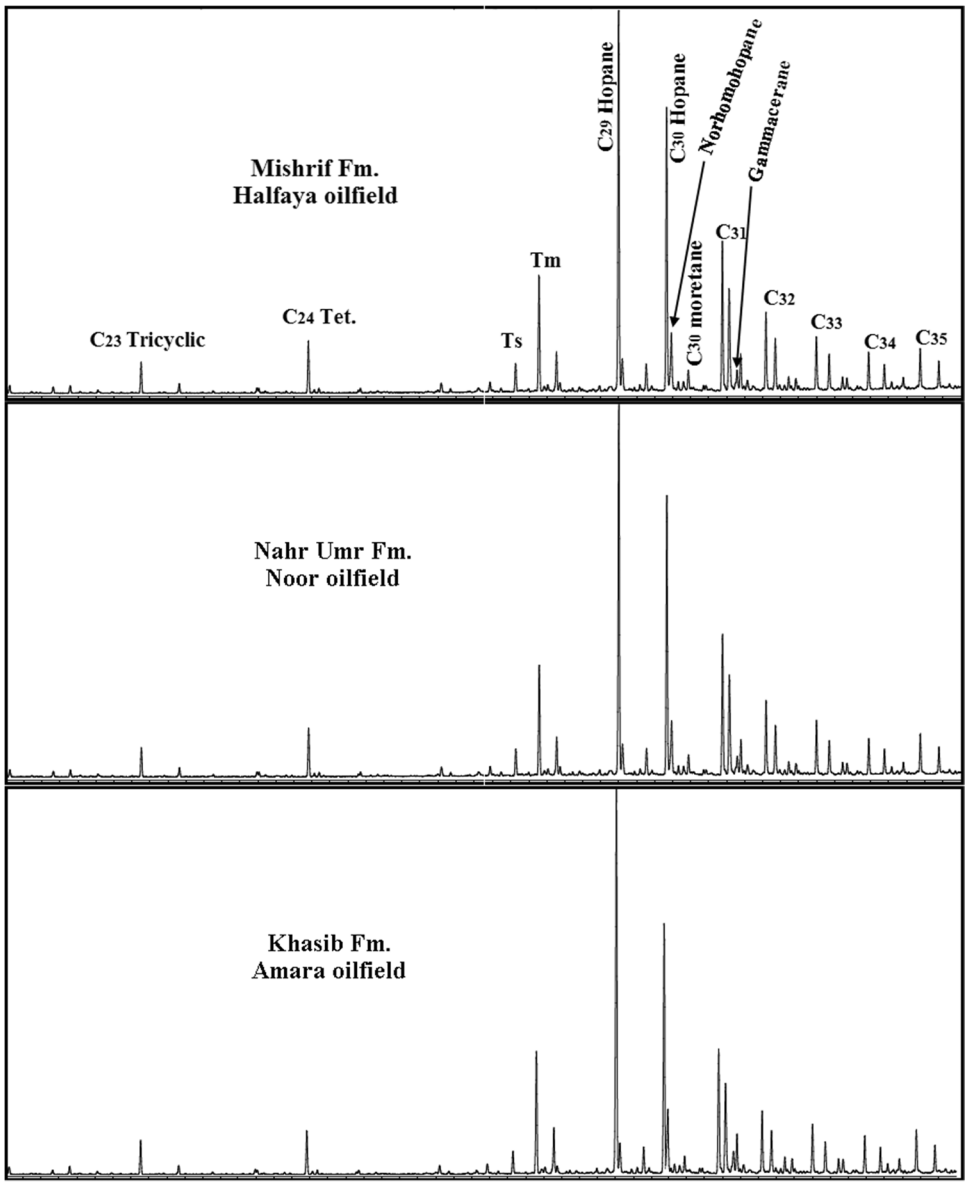

Fig. 8 *M/z* = 191 traces showing terpane distributions for some Halfaya, Amara, and Noor oil samples

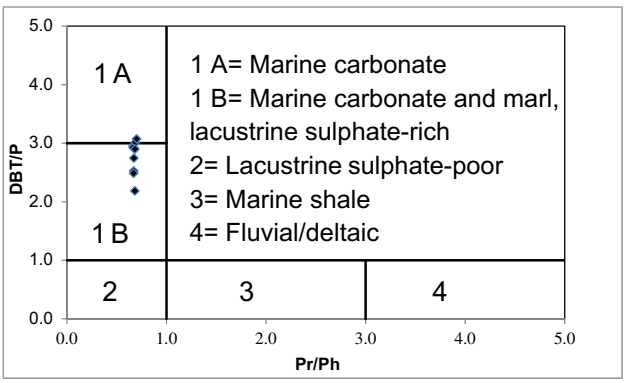

Fig. 9 Dibenzothiophene/phenanthrene versus pristane/phytane of the oil samples (Hughes et al. 1995) shows the oils were generated from marine carbonate and marl lacustrine sulfate-rich source rocks

chains is the suggested mechanism for the pregnane enrichment (Wang et al. 2010). Distributions of the triaromatic steroid (*m/z* 231) for the oil samples are consistent with the regular sterane distributions. The oils show enrichment of C_{20} and C_{21} triaromatic steroids relative to C_{26}–C_{28} compounds (Fig. 11) and abundant pregnane and homopregnane. This suggests that steranes and triaromatic steroids have a common source (Wang et al. 2010).

Thermal maturity

We estimated the thermal maturity of the nine oil samples in Table 4 using the sequential bracketing method described in Peters et al. (2005) and Peters and Moldown (2017). The C_{32} hopane 22S/(22S + 22R) ratio is controlled by a comparatively fast isomerization reaction and rises from

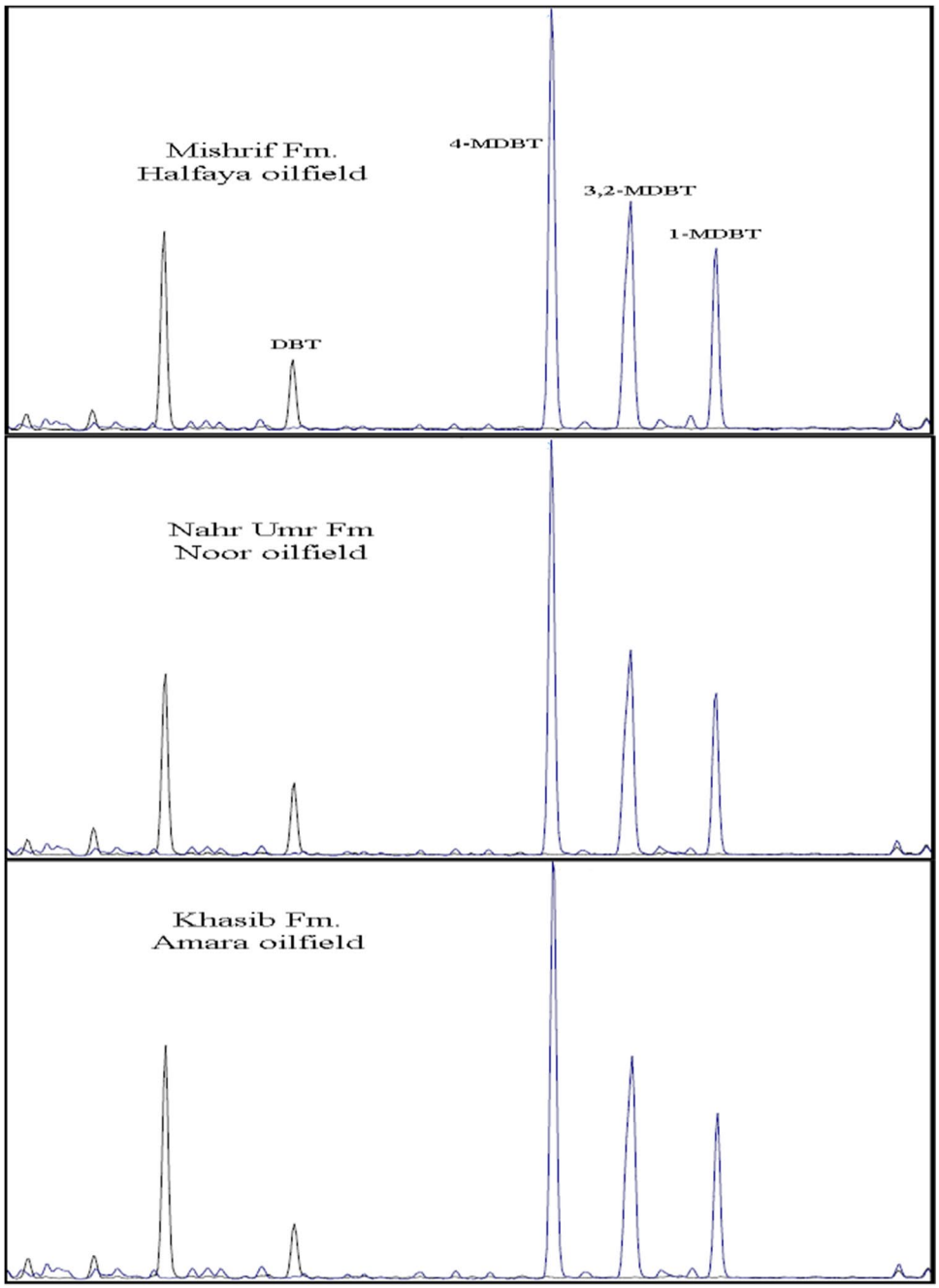

Fig. 10 Dibenzothiophene (DBT) and methyldibenzothiophene (MDBT) distributions for some oil samples

0 to ~ 0.6 (0.57–0.62: endpoint) during early maturation. The nine samples show 22S/(22S + 22R) ratios in the range 0.50–0.54, which indicates they have maturity *at least* within the early oil window (~ 0.6% R_oE). The C_{30} moretane ratio [17ß,21α(H) moretanes divided by 17α,21ß(H) hopanes; M/H in Table 4] is a slower reaction than that represented by the 22S/(22S + 22R) ratio. Furthermore, M/H ratios in Table 4 indicate that the nine oil samples have maturity at least within the early part of peak oil window (~ 0.7% R_oE).

Isomerization at C_{20} in the C_{29} steranes is a slower reaction than that represented by M/H and it causes 20S/(20S + 20R) to rise with increasing maturity from 0 to about 0.5 (0.52–0.55: endpoint). In addition, C29 ßß/(αα + ßß) rise with maturity from near-zero to about 0.7 (0.67–0.71: endpoint) with increasing maturity. Although the measurement of sterane isomerization by GCMS is generally less accurate rather than by GCMSMS, the data in Table 4 show that both ratios have not yet reached the endpoint (< 0.9% R_oE).

The above results are consistent with the methylphenanthrene index values (MPI) (Radke 1988) for the nine oil samples in Table 4 that indicate maturity in the range 0.79–0.85% R_oE. Additional more robust maturity

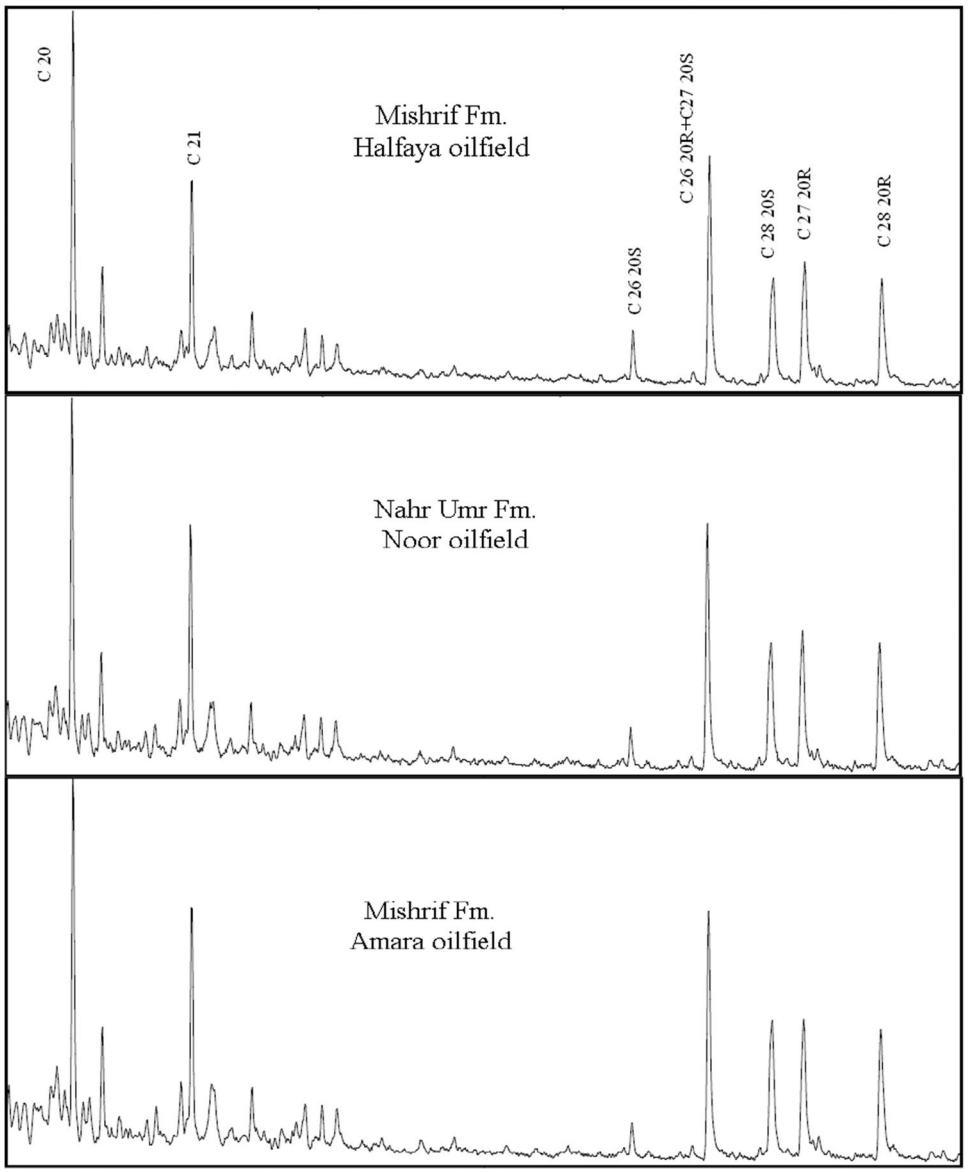

Fig. 11 *M/z* = 231 traces showing triaromatic steroid distributions for some southern Iraq oil samples

Table 4 Thermal maturity biomarker ratios for the oil samples

Well	Depth (m)	Oil family	M/H	C_{32} 22S/(S + R)	C_{29} S/(S + R)	C_{29} ββ/(αα + ββ)	MDR	MPI	VRc%
Noor-13	4123	1	0.07	0.52	0.42	0.57	2.44	0.71	0.80
Amara-6	3700	1	0.07	0.51	0.42	0.55	2.48	0.70	0.79
Amara-5	2820	1	0.07	0.51	0.42	0.56	2.48	0.70	0.79
Halfaya-18	3433	2	0.06	0.53	0.39	0.54	2.39	0.77	0.83
Halfaya-119	3130	2*	0.06	0.53	0.39	0.54	2.36	0.78	0.84
Halfaya-133	3445	2	0.06	0.53	0.40	0.54	2.38	0.76	0.83
Halfaya-272	3225	2	0.07	0.52	0.41	0.55	2.25	0.79	0.85
Noor-6	3473	2	0.06	0.52	0.39	0.54	2.38	0.78	0.84
Amara-5	2831	2	0.07	0.54	0.39	0.53	2.54	0.81	0.85

*Outliner in family 2; *M/H*, moretane/hopane; *MDR* (methyldibenzothiophene ratio), 4-MDBT/1-MDBT; *MPI*, 1.5(3-MP + 2-MP)/(P + 1-MP + 9-MP); *VRc%*, 0.6*MPI + 0.4

parameters, such as Ts/Tm, are not fully useful in this range of maturity but can be used to assess the late mature samples, where stereoisomerization ratios are ineffective because they have achieved endpoint.

It should be noted here that there are no systematic changes in the maturity of the oil samples with depth. All of the oils show similar maturity but migrated to reservoir at different depths.

Oil families

Chemometric analysis can be used to show genetic affinities among samples, better understand systematic relationships behind the data, and identify and remove noise from the data (He et al. 2012).

Based on biomarker data for the oil samples, the hierarchical cluster analysis (HCA) dendrogram identifies two oil families (Fig. 12A). Family 1 consists of two oils from Albian Nahr Umr and one from Cenomanian–Turonian Mishrif reservoirs from Noor and Amara oilfields, whereas

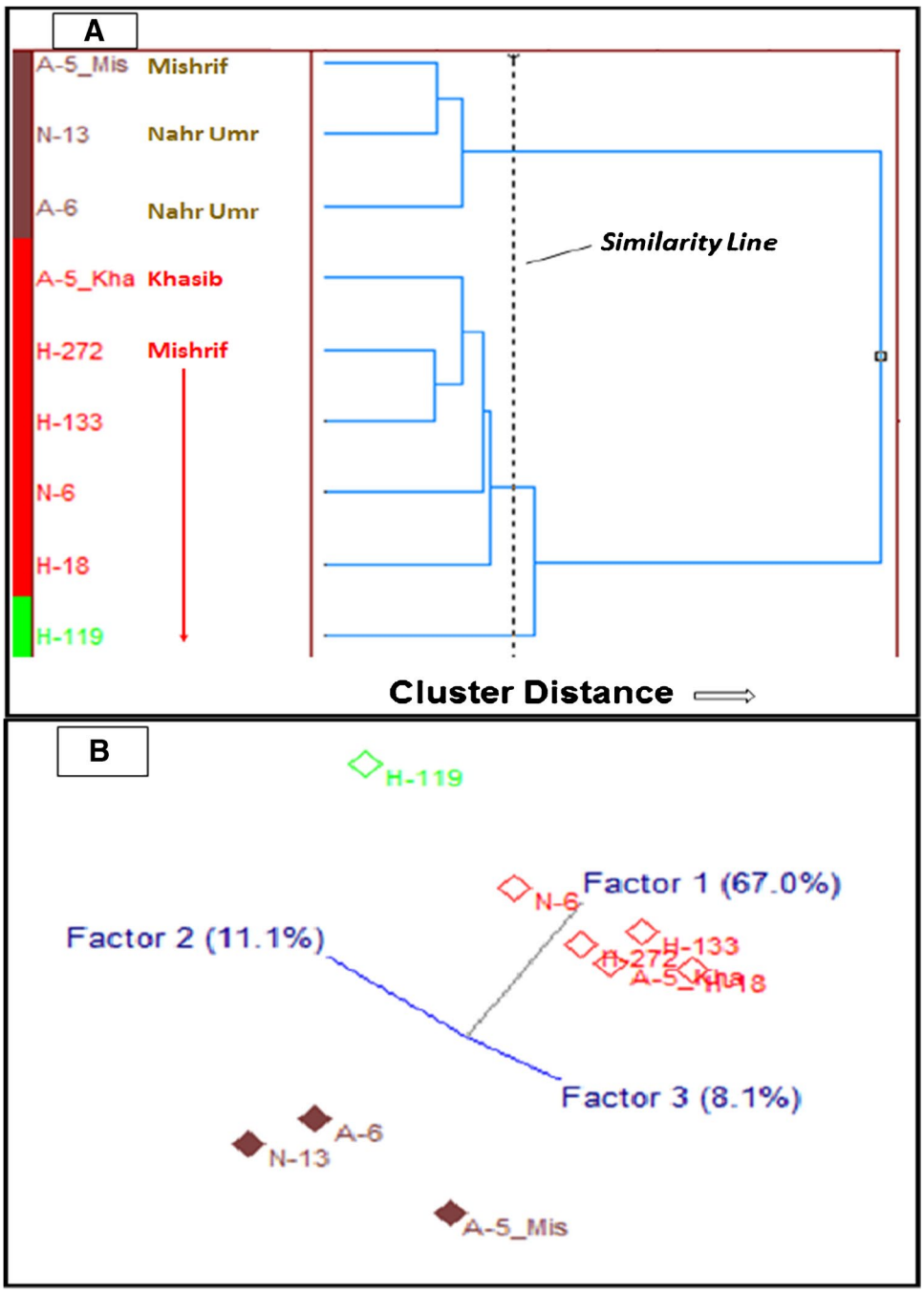

Fig. 12 **A** Hierarchical cluster analysis (HCA) for the Halfaya, Amara, and Noor oil samples. **B** Principal component analysis (PCA) shows distance between samples in eigenvector space where principal components 1 to 3 account for 86.2% of the variance in the data (see Tables 1–3 for sample information)

family 2 consists of five oils from Mishrif and Coniacian Khasib reservoirs in Halfaya, Noor, and Amara oilfields (Fig. 1). Oil H-119 is an outlier in family 2. To construct the HCA dendogram, fifteen parameters (two isotope and thirteen source-related biomarkers; Tables 1, 2, and 3) were used. These oil families may have originated from the same source rock, but with different organofacies. The parameters to differentiate the two oil families are listed in Tables 1, 2, and 3. Principal component analysis (PCA) (Fig. 12B) supports the HCA by identifying two oil families.

Compared to family 2, the oils in the family 1 are characterized by high content of low molecular-weight hydrocarbons ($< C_{15} = 32.02–34.74\%$) and saturated hydrocarbons (33.33–34.89%) and low content of polars (resins and asphaltenes) (23.55–26.54%) and sulfur (2.47–2.62%) (Table 1). In addition, they have relatively high values of *n*-C_{27}/*n*-C_{17} (0.21–0.22; Table 2), diasterane/regular steranes (0.20–0.21), streranes/hopanes (0.26), C_{24} tetracyclic terpanes/C_{23} tricyclic terpanes (1.68–1.69), C_{24}/C_{23} tricyclic terpanes (0.30–0.32), C_{19}/C_{23} tricyclic terpanes (0.17–0.19) and low values of C_{22}/C_{21} tricyclic terpanes (0.90–0.97), C_{30} norhomohopane/C_{30} hopane (0.18–0.19); gammacerane/C_{30} hopane (0.06–0.07), higher values of C_{29}/C_{30} hopane (1.32–1.34), Ts/Tm (0.24–0.25), and dibenzothiophene/phenanthrene (2.18–2.53) (Table 3), lightest carbon isotope values of whole oil (−27.63 to −27.46), saturated hydrocarbons(−28.23 to −28.12), and aromatic hydrocarbons (−27.53 to −27.52) (Table 1) compared to the oils of family 2. They also have the high values of the maturity biomarker ratios of C_{29} ββs/ααR and 20S/(S + R) (1.23–1.32 and 0.71–0.74 respectively, Table 4). These features indicate that oils of family 1 were more mature and were generated from carbonate source rocks with more clay input and algal organic matter, whereas oils of family 2 are less mature and also generated from carbonate source rocks, but with low clay content and high bacterial organic matter.

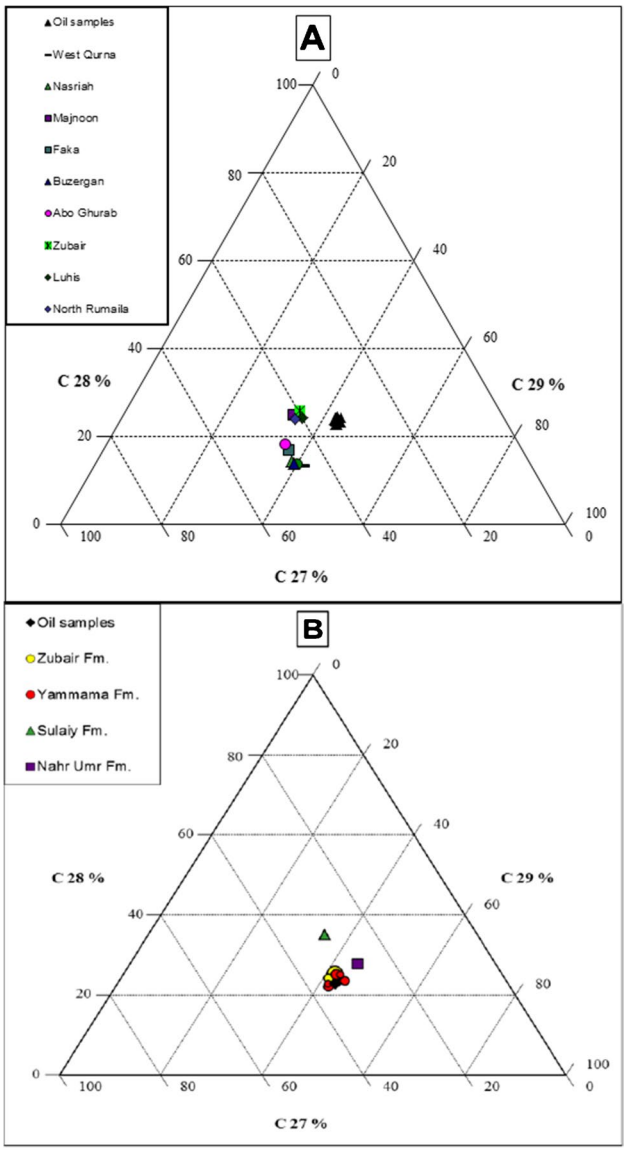

Fig. 13 Sterane ternary diagram for Halfaya, Amara, and Noor oil samples displays **A** oil groups with oil samples from some southern Iraq oilfields; **B** comparison with source rock extracts

Oil-oil correlation

As discussed above, it is evident that the oil samples from the Halfaya, Noor, and Amara oilfields, and most Iraq oils were generated from carbonate source rocks. However, sterane distributions of the present study oil samples (Fig. 13A) differ slightly from those of the Abu Gharab, Buzrgan, Faka, West Quran, Zubair, Majnoon, North Rumaila, and Luhais oils (Hakimi and Najaf 2016; Al-Khafaji et al. 2018; 2021). This suggests that the present study oils were generated from different organic matter. In addition, the oil samples of the present study are slightly more mature than other oils (Fig. 14). C_{29} sterane ββ/(ββ + αα) values of the oil samples is slightly higher than those for other oils, while moretane/hopane is slightly lower. Moreover, depositional environment ratios are also different (Fig. 15). Low gammacerane/C_{30} hopane values for the studied oils compared to other oil samples could indicate they were generated from source rocks deposited from a water column that lacked density stratification, with normal salinity. Pr/Ph values of the present study oils are lower than those of other oils, while $C_{35}S/C_{34}S$ values are higher, indicating that the present study oils were generated from source rocks deposited under more reducing condition than those for the other oils. On the other hand, Ts/Tm and diasteranes/regular sterane values for all oil samples are similar (Fig. 16), indicating that all oils were generated from similar facies. This could indicate that the oils were generated from similar source rocks having different depositional environment conditions. This interpretation

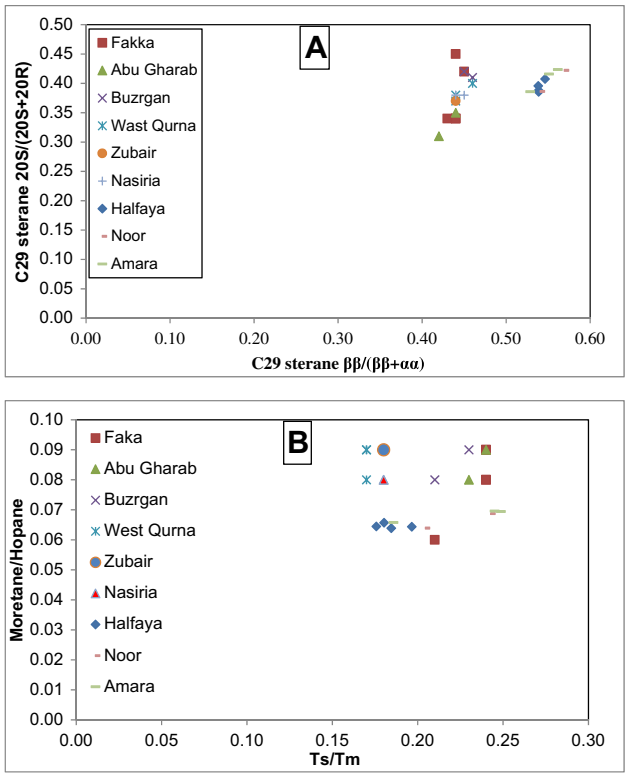

Fig. 14 **A** Plot of C_{29} sterane 20S/(20S + 20R) versus ββ/(ββ + αα); **B** Moretane/hopane versus Ts/Tm for the oil samples and oils from some southern Iraq oilfields, displays maturity levels

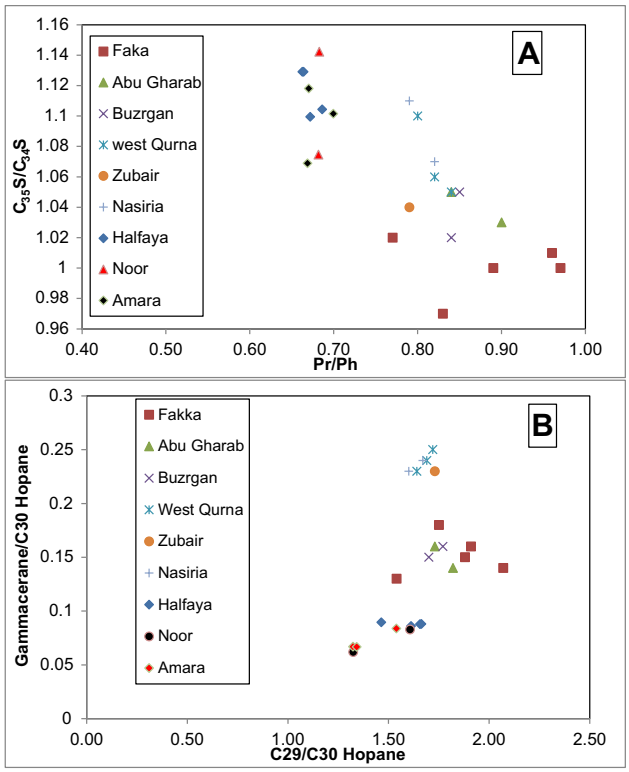

Fig. 15 **A** $C_{35}S/C_{34}S$ hopane versus pristane/phytane; and **B** Gammacerane/C_{30} hopane versus C_{29}/C_{30} hopane for the oil samples and oil of some southern Iraq oilfields; displays environment conditions

is supported by geologic evidence, where the successions become thicker in northeast direction toward the basin center (Fig. 2). This change may reflect changes in organofacies or conditions in the depositional environment.

Oil-source rock correlation

Because the rock samples for the potential source rocks were not available for analysis, the determination of the potential source rocks is speculative. To better understand the source rock depositional environment, the data from this study were compared with the published data on source rock and oils from the Mesopotamian Basin.

The main potential source rocks in southern Iraq are Middle Jurassic-Lower Cretaceous Sargelu, Sulaiy, Nahr Umr, Ratawi, Zubair, and Yamama formations (Jassim and Al-Gailani 2006; Abeed et al. 2011; Abdula 2020). According to basin modeling results for the Halfaya Oilfield (Al-Marsomy and Al-Ameri 2015), the Nahr Umr and Shuaiba formations are thermally immature, and therefore, they are excluded as source rocks at that location. The Ratawi Formation is clastic facies that contain mainly type III kerogen where hydrogen indices (HI) are generally low (45–188 mg HC/g TOC in Rumaila and Zubair oilfields) (Abeed et al. 2011);

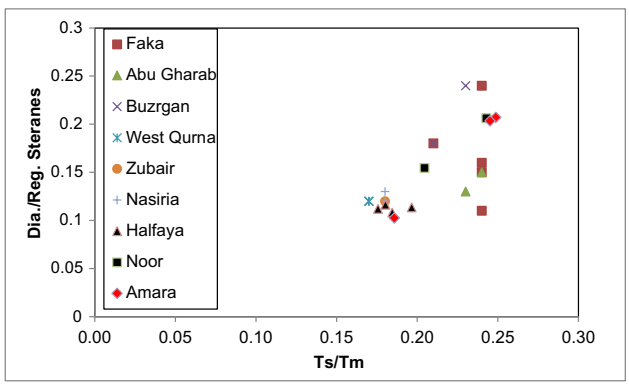

Fig. 16 Plot of diasterane/regular steranes versus Ts/Tm for the oil samples and oil from some southern Iraq oilfields; indicates similar lithofacies

therefore, it has low potential for oil generation. Zubair Formation has high TOC values (up to 32 wt%) and contains types III, mixed II/III, and II kerogen. It is early-mid-mature in southern Iraq, and it is considered the source rocks for oils of Zubair oilfield in southern Iraq (Idan et al. 2015). Basin modeling results indicate that Ratawi and Zubair formations are mature in the Halfaya Oilfield (Al-Marsomy

and Al-Ameri 2015). In addition, there is no indication for a significant contribution from terrigenous organic matter. Therefore, these formations cannot be considered significant source rocks for the analyzed oils, although some contribution from these formations cannot be excluded.

The Yamama and Sulaiy formations are mature in the Halfaya Oilfield (Al-Marsomy and Al-Ameri 2015) and are the most likely candidates as source rocks for the study oils. Sulaiy Formation rocks have a good source potential in southern Iraq. It consists mainly of carbonate with rare shale beds (Jassim and Buday 2006a, b, c, d). TOC values are in the range 0.1–7.3 wt% (average 2.8%) (Al-Ameri et al. 2009) and up to 9.5 wt% (Abeed et al. 2011). Sulaiy Formation shows mature vitrinite reflectance (1.0–1.4%) and hydrogen indices in the range 46–305 with an average 115 mg HC/g TOC and type II-S kerogen (Abeed et al. 2011). In Missan Province, it contains type II kerogen (Al-Musawi 2010). The Yamama Formation contains mature type II-S kerogen composed of amorphous organic matter with high HI values (140–598 mg HC/g TOC) (Abeed et al. 2011). In southern Iraq, Yamama consists of argillaceous and oolitic limestone deposited in an outer shelf environment (Jassim and Buday 2006a, b, c, d). Moreover, regular sterane distributions for the study oil samples are close to those of Sulaiy, Yamama, and Zubair extracts (Fig. 13B). These results may indicate that these formations are the source rocks for the Halfaya, Amara, and Noor oilfields. This assumption is consistent with the biomarker study, which suggests that the analyzed oils were generated from carbonate source rocks containing mainly type II or type II-S kerogen, with minor contributions from shales, and deposited under reducing marine conditions.

According to basin modeling results, Middle Jurassic source rocks are highly mature (R_o values in the range 1.2–1.9%) in the east margin of the Mesopotamian Basin and decrease systematically westward to about 0.6% R_o. At present, most of these source rocks reached or exceeded peak oil generation (Pitman et al. 2004). Oil generation started in the Late Cretaceous and was completed in the Late Paleogene (Pitman et al. 2004). Unfortunately, there are no published data on characteristics of the Middle Jurassic source rocks in southern Iraq. Based on the C_{28}/C_{29} sterane ratio, the Sargelu Formation considered the source rock in the Halfaya, Amara, and Noor oilfields (Al-Ameri et al. 2014; Hasan and Al-Dulaimi. 2017; Abdula 2020). The Sargelu Formation is one of the most important source rocks in northern Iraq (Al-Ameri et al. 2013; Abdula 2015; Sachsenhofer et al. 2015; Alkhafaji et al. 2020, 2021; Alkhafaji 2021). As discussed above, these oils are mid-mature and the Sargleu Formation is highly mature in the Mesopotamian Basin. In addition, the deepest oil reservoir in the Halfaya Oilfield is the Yamama Formation, which directly overlies the Sulaiy Formation. Therefore, the Yamama Formation overlies a thick interval represented by the Najmah, Gotnia, and Sulaiy formations (> 1000 m). The interval between the two formations consists of about 820 m of evaporites (Gotnia) and carbonates (Najmah), which limits mixing of oils generated from the Sulaiy and Sargelu source rocks.

Migration of oils from the Jurassic source rocks to Cretaceous reservoirs was dominantly vertical, and therefore, oil fields in the Mesopotamian Basin are located directly over the area of petroleum charge. Lateral migration is generally updip from east to west, but complex facies relations limited the lateral migration to short distances (Pitman et al. 2004). The Najmah Formation has good reservoir characteristics in southern and central Iraq (Sadooni 1997). Therefore, if the generated and expelled oils from the Sargelu Formation migrated vertically, then they should be reservoired, at least partly, in the Najmah Formation. According to Al-Ameri et al. (2014), the Najmah and Gotnia formations in the Halfaya oilfield lack oil shows. Moreover, Gotnia evaporites, which represent good seal rock in southern Iraq, are thick (402 m) in Halfaya Oilfield and have no fractures in the Basra area (Abeed et al. 2013). Therefore, these facts suggest that the Sagelu Formation is not the main source rock for the Halfaya, Noor, and Amara oilfields.

Conclusions

Oils from the Halfaya, Noor, and Amara oilfields belong to two oil families. These oil families may have originated from the same source rock, but with different organofacies. These oils and oils from the neighboring oilfields in southern Iraq were generated from similar facies, but with different depositional environment conditions. The most likely source rocks for the oils of this study are the Upper Jurassic-Cretaceous Sulaiy, Yamama, and Zubair formations. Therefore, extensive studies about the depositional environment condition, facies, and organofacies changes of the source rocks in the Mesopotamian Basin are recommended.

Acknowledgements We thank the Messan Oil Company (Amara) for providing the oil samples of this study; and Alex Zumberge at GeoMark Research for carrying out the biomarker analyses.

Author contribution Mohamed Waggaa Alkhafaji and Kenneth Peters took the lead in interpretation the results and writing the manuscript. Sawsan Faisal Al-Hazaa contributed to sample collection and contributed to the interpretation of the results.

Data availability Available on request.

Code availability Not applicable.

Declarations

Conflict of interest The authors declare no competing interests.

References

Abdula RA (2010) Petroleum source rock analysis of the Jurassic Sargelu Formation, northern Iraq. Master thesis. Colorado School of Mines, Golden, Colorado, 106 p

Abdula RA (2015) Hydrocarbon potential of Sargelu Formation and oil- source rock correlation, Iraqi Kurdstan. Arab J Geosci 8:5845–5868

Abdula RA (2020) Crude oil classification based on age and provenance from the southern Iraq: review. Bull Geol Soc Malays 70:87–102

Abeed Q, Al-Khafaji A, Littke R (2011) Source rock potential of the Upper Jurassic-Lower Cretaceous succession in the southern Mesopotamian Basin, Southern Iraq. J Pet Geol 34:117–134

Abeed Q, Leythaeuser D, Littke R (2012) Geochemistry, origin and correlation of crude oils in Lower Cretaceous sedimentary sequences of the southern Mesopotamian Basin, southern Iraq. Org Geochem 46:113–126

Abeed Q, Littke R, Strozyk F, Uffmann AK (2013) The Upper Jurassic- Cretaceous petroleum system of southern Iraq: a 3-D basin modeling study. GeoArabia 18:179–200

Al-Ameri TK, Al-Khafaji AJ, Zumberge J (2009) Petroleum system analysis of the Mishrif reservoir in the Ratawi, Zubair, North and South Rumaila oil fields, southern Iraq. GeoArabia 14:91–108

Al-Ameri TK, Al-Musawi FA (2011) Hydrocarbon generation potential of the uppermost Jurassic-basal Cretaceous Sulaiy Formation, South Iraq. Arab J Geosci 4:53–58

Al-Ameri TK, Najaf AA, Al-Khafaji AJ, Zumberge J, Pitman J (2013) Hydrocarbon potential of the Sargelu Formation, North Iraq. Arab J Geosci 6:3725–3735

Al-Ameri TK, Al-Marsoumi ShW, Al-Musawi FA (2014) Crude oil characterization, molecular affinity, and migration pathways of Halfaya oil field in Mesan Governorate, South Iraq. Arab J Geosci 8:7041–7056

Al-Khafaji AJ, Hakimi MH, Najaf AA (2018) Organic geochemistry characterisation of crude oils from Mishrif reservoir rocks in the southern Mesopotamian Basin, South Iraq: Implication for source input and paleoenvironmental conditions. Egypt J Pet 27:117–130

Al-Khafaji AJ, Hakimi MH, Mohialdeen MJ, Idan RM, Afify WE, Lashin AA (2021) Geochemical characteristics of crude oils and basin modelling of the probable source rocks in the Southern Mesopotamian Basin. South Iraq. J Pet Sci Eng 196:107641

Alkhafaji MW, Aljubouri ZA, Aldobouni IA, Littke R (2015a) a) Hydrocarbon potential of Ordovician-Silurian successions in Akkas field, western desert of Iraq. AAPG Bull 99:617–637

Alkhafaji MW, Aljubouri ZA, Aldobouni IA (2015b) b) Depositional environment of the Lower Silurian Akkas hot shales in the Western Desert of Iraq: results from an organic geochemical study. Mar Pet Geol 64:294–303

Alkhafaji MW (2017) Organic petrology of Ora Formation in Akkas field, western Iraq. Tikrit J Pure Sci 22:76–82

Alkhafaji MW (2018) Paleodepositional environment and hydrocarbon potential of Ora Formation, north and west Iraq. Diyala J Pure Sci 14:12–24

Alkhafaji MW, Al-Jubouri MA, Al-Miamary FA, Connan J (2020) Biodegradation and the origin of surface bitumens in the Palaeocene Kolosh Formation. Northern Iraq Arab J Geosci 13:554

Alkhafaji MW (2021) Biomarker assessment of oil biodegradation, water washing, and source rock characteristics of oil seeps from the foothill zone along the Tigris River. Northern Iraq. J Pet Sci Eng 197:107946

Alkhafaji MW, Connan J, Engel MH, Al-Jubouri SW (2021) Origin, biodegradation, and water washing of bitumen from the Mishraq Sulfur Mine, northern Iraq. Mar Pet Geol 124:104786

Al-Marsomy ShW, Al-Ameri TK (2015) Petroleum system modeling of Halfaya oil field south of Iraq. Iraqi J Sci 56:1446–1456

Al-Musawi FAS (2010) Crude oil characterization and source affinities of Missan oil fields, southeastern Iraq. PhD thesis, College of Science, University of Baghdad, p 177

Al-Nqar KRA, Faisal SH, Al-Jwaini YSK (2019) Microfacies analysis of the Mishrif and Kifil formations of Amara oil field, /south of Iraq. Tikrit J Pure Sci 24:45–54

Alsharhan AS, Nairn AEM (1997) Sedimentary basins and petroleum geology of the Middle East. Elsevier, The Netherlands, p 843

Ameen MS (1992) Effect of basement tectonics on hydrocarbon generation, migration, and accumulation in northern Iraq. AAPG Bull 76:356–370

Aqrawi AAM, Goff JC, Horbury AD, Sadooni FN (2010) The petroleum geology of Iraq. Scientific Press Ltd., Beaconsfield, United Kingdom, p 424

Bray EE, Evans ED (1961) Distribution of n-paraffins as a clue to recognition of source beds. Geochim Cosmochim Acta 22:2–15

Burton ZFM, Moldowan JM, Magoon LB, Sykes R, Graham SA (2019) Interpretation of source rock depositional environment and age from seep oil, east coast of New Zealand. Int J Earth Sci 108:1079–1091

Clark JP, Philp RP (1989) Geochemical characterization of evaporite and carbonate depositional environments and correlation of associated crude oils in the Black Creek Basin, Alberta. Bull Can Pet Geol 37:401–416

Didyk BM, Simoneit BRT, Brassell SC, Eglinton G (1978) Organic geochemical indicators of palaeoenvironmental conditions of sedimentation. Nature 272:216–222

Hakimi MH, Najaf AA (2016) Origin of crude oils from oilfields in the Zagros Fold Belt, southern Iraq: relation to organic matter input and paleoenvironmental conditions. Mar Pet Geol 78:547–561

Hasan ASN, Al-Dulaimi SI (2017) Crude oil characterization and hydrocarbon affinity of Amarah Oil Field, South Iraq. Iraqi J Sci 58:103–114

He M, Moldowan M, Nemchenko-Rovenskaya A, Peters KE (2012) Oil families and their inferred source rocks in the Barents Sea and northern Timan-Pechora Basin, Russia. AAPG Bull 96:1121–1146

Hughes WB, Holba AG, Dzou LIP (1995) The ratios of dibenzothiophene to phenanthrene and pristane to phytane as indicators of depositional environment and lithology of petroleum source rocks. Geochim Cosmochim Acta 59:3581–3598

Idan RM, Faisal RF, Nasser ME, Al-Ameri TK, Al-Rawi D (2015) Hydrocarbon potential of Zubair Formation in the south of Iraq. Arab J Geosci 8:4805–4817

Jassim SZ, Al-Gailani M (2006) Hydrocarbons. In: Jassim S. Z. and Goff J. C. (Eds.), Geology of Iraq: Brno, Prague, and Moravian Museum, pp. 232–250.

Jassim S Z, Buday T (2006a) Units of the Stable Shelf. In: Jassim S. Z. and Goff J. C. (Eds.), Geology of Iraq: Brno, Prague, and Moravian Museum, pp. 57–70.

Jassim S Z, Buday T (2006b) Tectonic framework. In: Jassim S. Z. and Goff J. C. (Eds.), Geology of Iraq: Brno, Prague, and Moravian Museum, pp. 45–56.

Jassim SZ, Buday T (2006c) Late Toarcian-Early Tithonian (Mid-Late Jurassic) Megasequence AP7. In: Jassim S. Z. and Goff J. C. (Eds.), Geology of Iraq: Brno, Prague, and Moravian Museum, pp. 117–123.

Jassim SZ, Buday T (2006d). Late Tithonian-Early Turonian Megasequence AP8. In: Jassim S. Z. and Goff J. C. (Eds.), Geology of Iraq: Brno, Prague, and Moravian Museum, pp. 124–140.

Jiang L, George SC (2020) Geochemical comparison of three oil families from the Gippsland Basin SE Australia. Mar Pet Geol 121:104575

Mohamed AKA (2021) Anomalous porosity preservation in the Lower Cretaceous Nahr Umr sandstone. Southern Iraq. Russ J Earth Sci 21:ES2001

Moldowan JM, Fago F, Lee CY, Jacobson SR, Watt DS, Slougui N, Jeganathan A, Young DC (1990) Sedimentary 24-*n*- propylcholestanes, molecular fossils diagnostic of marine algae. Science 247:309–312

Moldowan JM, Seifert WK, Gallegos EJ (1985) Relationship between petroleum composition and depositional environment of petroleum source rocks. AAPG Bull 69:1255–1268

Palacas JG (1984) Carbonate rocks as sources of petroleum: geological and chemical characteristics and oil-source correlations. Proceedings of the Eleventh World Petroleum Congress 1983, London 2, 31–43.

Peters KE, Moldowan JM (1991) Effects of source, thermal maturity, and biodegradation on the distribution and isomerization of homohopanes in petroleum. Org Geochem 17:47–61

Peters KE, Moldown JM (2017) Biomarker: assessment of thermal maturity. In White, W.M. (ed). Encyclopedia of Geochemistry. Springer International Publishing. https://doi.org/10.1007/978-3-319-39193-9-147-1

Peters KE, Moldowan JM (1993) The biomarker guide. Interpreting molecular fossils in petroleum and ancient sediments. Prentice Hall, Englewood Cliffs New Jersey, p. 363

Peters KE, Walters CC, Moldowan JM (2005) The biomarker guide, 2nd edn. Cambridge University Press, Cambridge, UK, p 1155

Pitman JK, Steinshouer D, Lewan MD (2004) Petroleum generation and migration in the Mesopotamian Basin and Zagros Fold Belt of Iraq: results from a basin-modeling study. GeoArabia 9:41–72

Radke M (1988) Application of aromatic compounds as maturity indicators in source rocks and crude oils. Mar Pet Geol 5:224–236

Requejo AG, Hieshima GB, Hsu CS, McDonald TJ, Sassen R (1997) Short chain (C_{21} and C_{22}) diasteranes in petroleum and source rocks as indicators of maturity and depositional environment. Geochim Cosmochim Acta 61:2653–2667

Rohmer M, Bisseret P, Neunlist S (1992) The hopanoids, prokaryotic triterpenoids and precursors of ubiquitous molecular fossils. In: Moldowan JM, Albrecht P, Philp RP (eds) Biological markers in sediments and petroleum. Prentice Hall, Englewood Cliffs, NJ, pp 1–17

Sachsenhofer RF, Bechtel A, Gratzer R, Rainer TM (2015) Source-rock maturity, hydrocarbon potential and oil- source-rock correlation in well Shorish-1, Erbil Province, Kurdistan Region, Iraq. J Pet Geol 38:357–382

Sadooni FN (1997) Stratigraphy and petroleum prospects of the Upper Jurassic carbonates in Iraq. Pet Geosci 3:233–243

Sinninghe Damste' JS, Kenig F, Koopmans MP, Koster J, Schouten S, Hayes JM, de Leeuw JW (1995) Evidence for gammacerane as an indicator of water column stratification. Geochim Cosmochim Acta 59:1895–1900

Sofer Z (1984) Stable carbon isotope compositions of crude oils: application to source depositional environments and petroleum alteration. AAPG Bull 68:31–49

Taha TM, Abdullah EJ (2020) Mineralogy and geochemistry of Mishrif Formation from selected oilfields, southeast of Iraq. Tikrit Journal of Pure Science 25:75–84

Tissot BP, Welte DH (1984) Petroleum Formation and Occurrence. Second Edition. Springer Verlag, Berlin, p 699

Verma MK, Ahlbrandt TS, Al Gailani M (2004) Petroleum reserves and undiscovered resources in the total petroleum systems of Iraq: Reserve growth and production implications. GeoArabia 9:51–74

Volkman JK (1986) A review of sterol markers for marine and terrigenous organic matter. Org Geochem 9:83–99

Volkman JK (2003) Sterols in microorganisms. Appl Microbiol Biotechnol 60:496–506

Volkman JK, Barrett SM, Blackburn SI (1999) Eustigmatophyte microalgae are potential sources of C_{29} sterols, C_{22}–C_{28} *n*-alcohols and C_{28}–C_{32} *n*-alkyl diols in freshwater environments. Org Geochem 30:307–318

Wang Z, Fingas M (1995) Use of methyldibenzothiophenes as markers for differentiation and source identification of crude and weathered oils. Environ Sci Technol 29:2842–2849

Wang G, Wang T-G, Simoneit BRT, Zhang L, Zhang X (2010) Sulfur-rich petroleum derived from lacustrine carbonate source rocks in Bohai Bay Basin, East China. Org Geochem 41:340–354

Waples DW, Machihara,T (1991) Biomarkers for geologists: A practical guide to the application of steranes and triterpanes in petroleum geology. Am Assoc Pet Geol Methods Explor Ser 9:91

Zumberge JE (1984) Source rocks of the La Luna (Upper Cretaceous) in the Middle Magdalena Valley, Colombia. In: Palacas, J.G. (Ed.), Geochemistry and source rock potential of carbonate rocks. American Association of Petroleum Geologists, Tulsa, OK, pp. 127–133